Laser and Particle Beams (2014), *32*, 455–460.

doi:10.1017/S026303461400038X

Proton activation history on the Vulcan high-intensity petawatt laser facility

R.J. CLARKE, S. DORKINGS, R. HEATHCOTE, K. MARKEY, AND D. NEELY
Central Laser Facility, STFC Rutherford Appleton Laboratory, Harwell Oxford, Oxfordshire, United Kingdom
(RECEIVED 1 May 2014; ACCEPTED 18 June 2014)

Abstract

High-intensity lasers are an effective source for the acceleration of high-energy particles. Using different interaction configurations, such facilities can be optimized for the acceleration of electrons, protons, heavy ions, high-energy photons, or neutrons. The shielding of these facilities to ensure the safety of personnel has always been a critical requirement and is a fundamental step within the design phase. The knowledge of radiation source terms through both experiments and modelling is now well understood and for the most part can be dealt with through the use of shielding and specialized beam dumps. Unlike most other particle accelerators most high-power laser facilities are still accessed by personnel post shot with little or no remote handling capabilities. As a result, the secondary activation and control of components that lie around the interaction is of great importance to safety. In this paper, we present a 10 year history of activation data on the Vulcan petawatt facility and discuss the primary sources of activation and the potential impact on future laser facilities.

Keywords: Activation; Ion; Laser; Proton; Radiation

INTRODUCTION

The Vulcan Petawatt Facility (Hernandez-Gomez *et al.*, 2006) is a Nd:Glass laser system that uses optical parametric chirped pulse amplification system (Chekhlov *et al.*, 2006) to generate short pulse, high contrast laser pulses with energies up to 400 J on target for high-intensity plasma physics experiments. The facility operates with a parabolic $f/3$ focusing optic to reach intensities of up to 10^{21} W/cm^2 and typically fires to target at a rate of 1 shot every 45 minutes. At these intensities, the laser-target interaction can be optimized for the production of hundreds of MeV electrons (Kneip *et al.*, 2011) using gas jets (Azambuja *et al.*, 1999), tens of MeV photons (Ledingham *et al.*, 2000) using thick solid targets, MeV neutrons using deuterated targets, and protons/ions of tens of MeV per nucleon (Robson *et al.*, 2007). All of the accelerated particles/radiation has the capability to generate activity within the components surrounding the laser-target interaction, the experimental vacuum chamber and potentially the target area itself. For many experiments, the secondary activation of sample foils is often used for diagnosing the radiation/particle flux and directionality (Clarke *et al.*, 2006) since the isotope can often be identified and the exact source of radiation characterized (Clarke *et al.*, 2008; Gunther *et al.*, 2013).

As part of the inherent safety systems in place at the Vulcan Facility, activation monitoring, material logs, and control of activated materials have been in place since the start of operations in 2002. Over this period, 46 experiments were undertaken and almost 3000 high power laser shots delivered to target. Dose rates from active components are measured using Thermo Scientific Mini 900D dose rate monitors. Typically, 3–4 laser shots are taken before the interaction chamber is let up from vacuum to atmosphere. Access to the interaction chamber can be achieved within 15 minutes following the last shot.

Most of the produced radiation is emitted into divergent beams with cone angles typically of tens of degrees. With the benefit of the inverse square law, no measurable dose rates (above 0.2 μSv/hr on contact) have been measured outside of about 0.5 m radius around the laser-target. Within this 0.5 m sphere, a typical shot run will see the activation of multiple components. Activated components are removed where possible and logged for time and current dose rate. Identification of nuclides is performed (where unknown) through either gamma spectroscopy using a high purity germanium

Address correspondence and reprint requests to: Robert J Clarke, STFC Rutherford Appleton Laboratory, Experimental Science Group, Harwell Oxford, Didcot, Oxfordshire OX11 0QX, United Kingdom. E-mail: rob.clarke@stfc.ac.uk

detector, sodium iodide scintillators in either single or coincidence mode or simply through half-life measurements. Irradiating radiation/particles can be identified through the likely transitions such as (p, n), (γ, n), (n, ǹ), or in many cases simply by the positioning with respect to targets — for example, in ion acceleration experiments dominated by target normal sheath acceleration (Carroll *et al.*, 2008) proton activation is expected along the target normal. Analysis of the data obtained throughout the operational history demonstrates that almost all components with measurable dose rates are derived from proton activation.

With a high-energy laser source of several hundred Joules, total proton yields can easily exceed 10^{14} protons with over 10^{10} protons at energies above 8 MeV where the primary (p, n) reaction cross-section peaks typically occur. This represents an overall conversion efficiency of up to 15% into protons (Brenner *et al.*, 2014). The primary (p, n) reactions dominate the observed activation, but higher energy reactions such as (p, *x*n) and (p, n + p) are also commonly observed and provide a small contribution to induced activities. Since not all experiments generate a substantial proton yield many experiments produce little or no activated products — gas/cluster targets, thick solid targets (Yuan *et al.*, 2010), double pulse configurations etc. The compiled 10 cm dose rate (μSv/hr) measured at 10 cm for activated components can be seen in Figure 1. The time stamped data supports the proton activation hypothesis, since activated data appears only in clusters around specific experiments.

In-chamber handling procedures have been developed to reduce accessible dose rates as far as practicably achievable. This requires the constant monitoring of accessible dose rates and understanding the route of activation. Where possible, these routes are removed but this is not always practical.

ANALYSIS

The activated components are allocated into one of two main categories — (1) experimental samples and (2) machine components. The contribution to dose rates greater than 10 μSv/hr at 10 cm on accessing the interaction chamber is shown in Figure 2.

Experimental Samples

Mapping of the spatial and energy distribution of accelerated protons is critical to many of the ion acceleration experiments performed at the facility and there are only a few techniques available for single shot measurements. The two main sample types used to diagnose the emitted proton beams — "Radiochromic/Gafchromic film" and "Activation stacks." Radiochromic film (Nurnberg, 2009) is a dose sensitive film that changes color to represent the level of dose to which it is exposed. This is commonly used to provide a

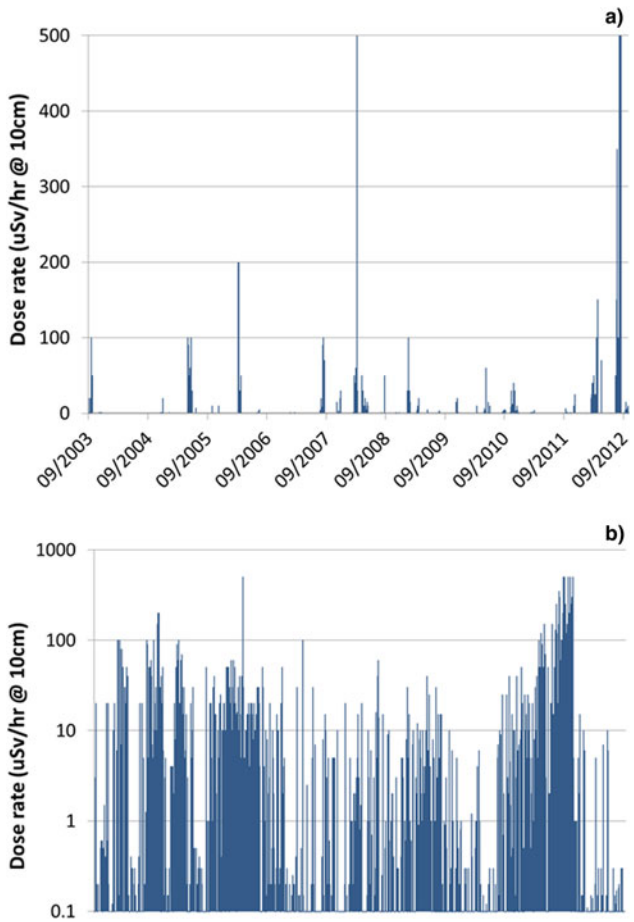

Fig. 1. (Color online) Measured dose rates from chamber activated components on the Vulcan petawatt facility, August 2003 – December 2012 plotted as (**a**) time stamped and (**b**) individual items.

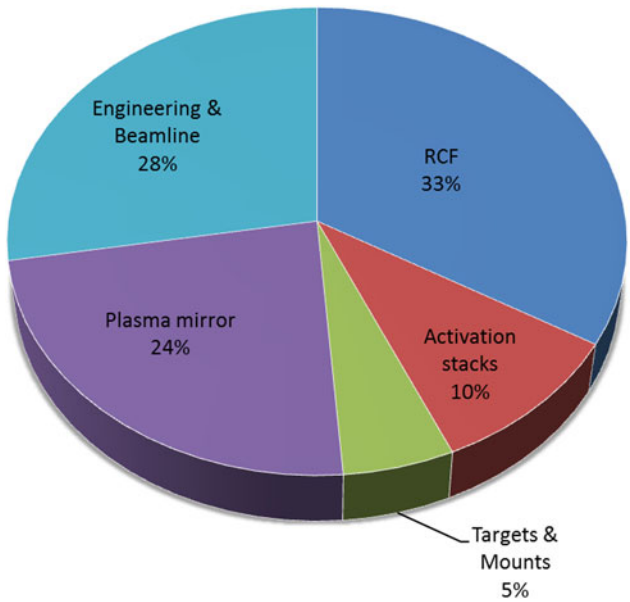

Fig. 2. (Color online) Breakdown of activated components less than 10 μSv/hr at 10 cm from the Vulcan petawatt facility, based on category type over the entire period.

https://doi.org/10.1017/S026303461400038X Published online by Cambridge University Press

spatial profile of the emitted particle beams at multiple energies. When exposed to high levels of protons, ^{13}N is also produced within the plastic substrate, with a half-life of 9.97 minutes and is one of the most commonly observed products. The activation stacks are used for determining absolute proton spectra, typically through the ^{63}Cu (p, n) ^{63}Zn reaction with a half-life of 38.5 minutes (Santala *et al*., 2001) and are often used in conjunction with the Radiochromic/Gafchromic film. The only steps available to minimize the produced activation is by using thin materials or where stacks are required for energy measurement through depth penetration, the use of separating filters with either very long or very short half-lives.

Machine Components

Machine components are the components and equipment required to either deliver the laser beam to target or to diagnose the laser-target interactions and are not intentionally activated. This category is subdivided into three — "targets and mounts," "plasma mirrors," and "engineering and beamline." The first category contains any equipment directly associated with the target and its mounting. Plasma mirrors (Ziener *et al*., 2003) are glass substrates used to provide an enhancement of the laser pulse contrast. All other items, such as experimental and opto-mechanical equipment, diagnostic mounting, and general optics are included in the engineering and beamline category. Initially, most of the activation observed in this category was through the activation of stainless steel components such as opto-mechanical posts/pillars and bolts. These typically become active through the ^{52}Cr (p, n) ^{52m}Mn reaction with a half-life of 21.1 minutes. The typical concentration of chromium within a stainless steel component is on the order of 10–15% with almost all of this (84%) being ^{52}Cr. Where possible, components are removed from the proton emission cone or substituted with custom aluminum components. The resultant activation of the aluminum is dominated by the ^{27}Al (p,n) ^{27}Si reaction with half-life of about 4 seconds. This rapidly decays before the chamber is accessible and hence accessible dose rates are negligible. Where neither of these is possible, aluminum shielding is used to moderate the protons to energies below the cross-section thresholds. In cases where substitution or shielding are simply not possible and components cannot be extracted for storage, administrative controls are used to restrict working around these components. In recent years, the greatest contribution to the accessible doses has been through the use of plasma mirrors. These are disposable optics used to improve the laser contrast by generating a "switch-on" of the mirror part way into the rising edge of the main laser pulse. On smaller scale laser systems, a dedicated plasma mirror system can be installed part way through the beam propagation but as the beam diameter increases this becomes more intrusive. In these

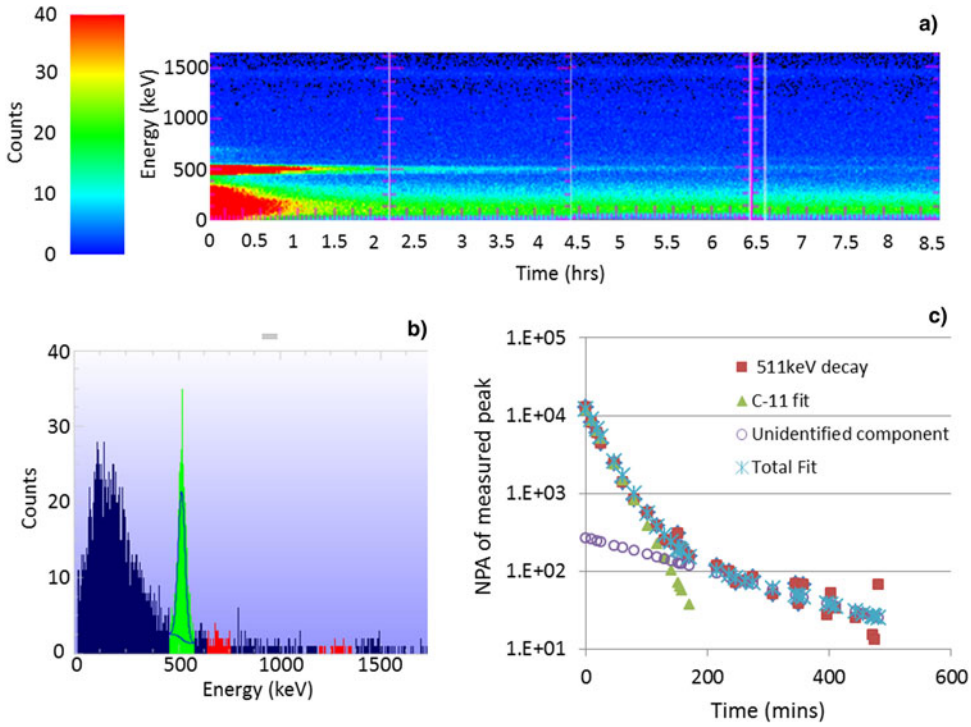

Fig. 3. (Color online) Measured decay products from an activated plasma mirror from Target Area Petawatt. Data is taken using a Scionix 2" NaI detector coupled to a Canberra Osprey MCA running in multi-spectral scaling mode. (**a**) Multi-spectral scaling buffer data showing full spectrum against elapsed time (from measurement start), (**b**) snapshot of the spectrum showing the 511 keV peak from the β+ decay, and (**c**) plotted net peak area of the 511 keV decay with associated fit for the ^{11}C decay and a presently unidentified component with an approximate half-life of 2.3 hours.

https://doi.org/10.1017/S026303461400038X Published online by Cambridge University Press

cases, the plasma mirrors are used close (within a few cm's) to target after the main focusing optic. In such circumstances, the plasma mirror substrate is likely to be within the proton emission cone and at such close proximity to the target has a potential for high activation. Borosilicate glass (BK7) or equivalent is the typical material used at present for these components. The boron content is around 10% and ^{11}C is generated through the ^{11}B (p,n) ^{11}C reaction with a half-life of 20.4 minutes. A typical example of plasma mirror activation can be seen in Figure 3. Accessible dose rates from plasma mirrors can approach several hundreds of μSv/hr at 10 cm and are required to be extracted and stored until appropriately decayed. With up to four exchanges per day this is currently within the capability of the facility without employing specialist remote handling but replacement of BK7 with a lower boron content glass is in progress to reduce accessible dose rates.

FACTORS FOR HIGH REPETITION FACILITIES

The development of high-intensity laser facilities continues to be rapid, and new facilities such as those for the extreme light infrastructure (http://eli-laser.eu/index.html) will begin to come online within the next few years. With a continually evolving physics program, many of these facilities will achieve the same level of single-shot activation as the current Vulcan facility, but at greatly increased shot rates. This is of major concern for the protection of personnel. As the shot repetition rate increases, the activated components begin to see repetitive activation before they have significantly decayed. This leads to activation build-up, and continues to increase until the "saturation regime" is reached where the decay between shots is equivalent to the activity generated by the following shot. In addition, low level impurities which currently do not significantly contribute to exposure levels become an important factor for high repetition rates. To demonstrate this, Figure 4 plots the (p,n) generated isotopes from both engineering grade aluminum (6082) and stainless steel as their relative cross-section (peak cross-section multiplied by the percent of the isotope present) against the isotope half-life. This creates a map on which the area of concern for personnel exposure can be drawn. For the Vulcan facility, this is in the region of relative cross-section less than 1×10^{-3} mbarn and a half-life between 1 minute and 2–3 hours. More rapid half-lives decay prior to personnel being able to access the interaction chamber and longer half-life isotopes will have a very small emitted dose rate. Currently within this region there are no generated aluminum isotopes and only two from the stainless steel — the ^{52}Mn from the ^{52}Cr (p, n) ^{52m}Mn reaction discussed earlier and ^{54}Co from the ^{55}Fe (p, n) ^{54}Co reaction with a half-life of 1.48 minutes.

As the shot repetition rate increases, the potential build-up of activation pushes the region of concern to lower relative

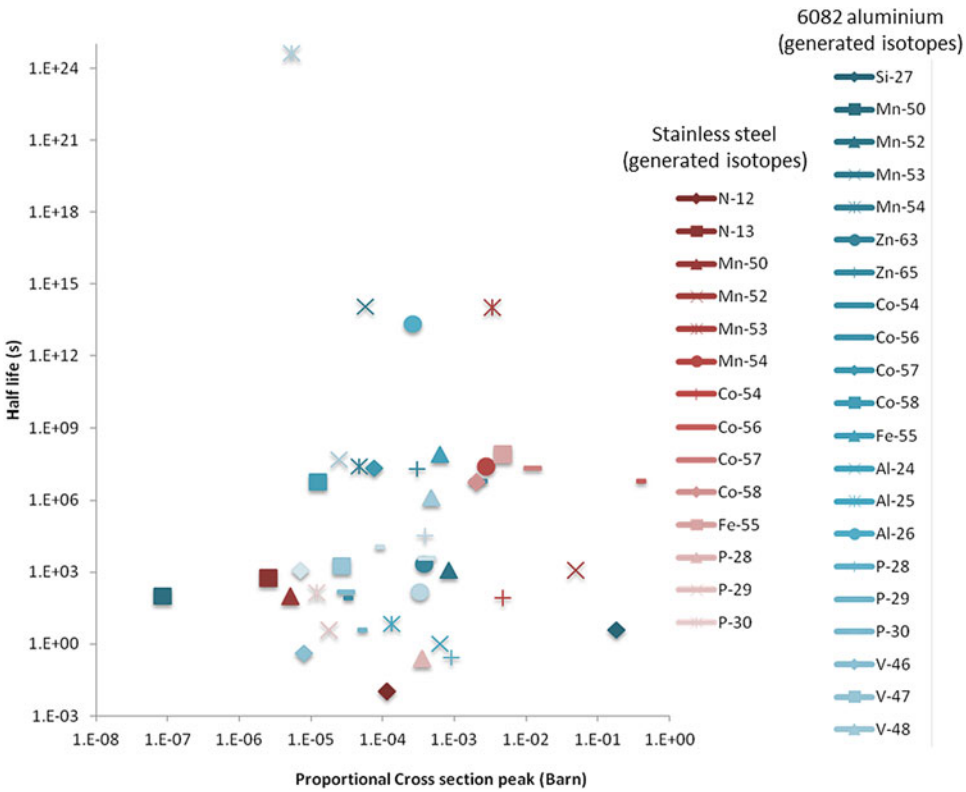

Fig. 4. (Color online) Generated isotopes through (p,n) reactions in stainless steel (red) and 6082 grade aluminum (blue) plotted as proportional peak cross-section against half-life.

https://doi.org/10.1017/S026303461400038X Published online by Cambridge University Press

cross-sections (almost proportional to the increase in shot rate) and also toward longer half-lives. Even looking at only these primary reactions, it is clear that for a high-repetition rate facility, the number of additional isotopes contributing to exposure (and as such the associated dose rates) are dramatically increased. The longer half-life components dominate the residual dose rates following the end of operations and will dictate the time before personnel can access the facility. Considering the level of contaminants in the engineering grade aluminum it is clear that an increase in repetition rate of a factor of 10^3 will bring a large number of isotopes to the activity level currently observed within stainless steel components through the ^{52}Cr (p, n) ^{52m}Mn reaction. This 10^3 increase only represents a repetition rate of 0.5 Hz. With almost 60% of all activated components observed on the current petawatt facility measuring greater than 1 μSv/hr at 10 cm, scaling to Hz repetition rates clearly poses a large increase in the radiation hazards to which personnel may be exposed. At such repetition rates it may no longer be possible to maintain safe operations through the substitution of materials or administrative controls and a full remote handling infrastructure may be required. The accidental exposure of components in such laser facilities becomes a significant risk and could bring future large scale laser facilities into the activation territory of large electron accelerators or pulsed neutron sources where component activities approaching PBq levels are commonly observed.

CONCLUSIONS

High-intensity laser facilities operating at intensities in the region of 10^{19}W/cm^2 or above can easily generate levels of activity that must be both monitored and controlled to mitigate unwanted exposure to personnel. The primary activation observed to date is generated through (p, n) reactions and is highly dependent upon the proton energies and numbers. Many of the most active materials have been found to be samples to which the experimental visitors want immediate access for data analysis and therefore stringent operational rules are required to control this material. However, the activation of machine components dominates the overall number of activated components as well as the highest dose rates, especially when employing plasma mirrors close to focus. The primary techniques for minimizing the levels of activity are through the substitution of materials in use — predominantly stainless steel (containing chromium), borosilicate glass (containing boron), plastics and copper, which are also present in brass components. The control of experimental configurations to minimize components within the emitted proton cones (presently dominated along target axis) is key to maintaining a minimum level of activation on both current facilities and planned upgrades.

Current high-intensity laser systems can be operated with relatively simple controls to prevent or control unwanted exposure but the future position of large facilities is not quite as clear. As facilities are developed to produce higher powers, intensities and/or energies, the immediate level of activation will potentially increase, and may eventually become comparable to that of facilities such as pulsed neutron sources or electron accelerators. As the proton and electron energies increase further, the potential for spallation and high-energy cascades also increases, putting further emphasis on neutron activation which currently contributes only a small proportion of the observed activities within laser facilities. Finally, the ever increasing repetition rate of high-intensity facilities poses a large concern for the build-up of activation. Significant activity is likely to be achieved through low level material impurities and the need for remote handling systems and even more stringent control of equipment and facility construction materials is required.

REFERENCES

Azambuja, R., Eloy, M., Figueira, G. & Neely, D. (1999). Three dimensional characterisation of high density non cylindrical pulsed gas jets. *J. Phys. D* **32**, L35–L43.

Brenner, C.M., Badziak, J., Batani, D., Davies, J.R., Deppert, O., Gray, R.J., Hassan, S.M., Lancaster, K.L., Li, K., Markey, K., Mckenna, P., Musgrave, I.O., Neely, D., Norreys, P.A., Pasley, J., Robinson, A.P.L., Rosinski, M., Roth, M., Schlenvoigt, H.-P., Scott, R.H.H., Spindloe, C., Tatarakis, M., Winstone, T., Wolowski, J. & Wyatt, D. (2014). High energy conversion efficiency in laser-proton acceleration by controlling laser-energy deposition onto thin foil targets. *Appl. Phys. Lett.* **104**, 081123.

Carroll, D.C., Bandyopadhyay, S., Batani, D., Bellei, C., Evans, R.G., Kar, S., Li, Y.T., Lindau, F., Lundh, O., Markey, K., Mckenna, P., Neely, D., Pepler, D., Redaelli, R., Simpson, P.T., Wahlstrom, C.-G., Xu, M.H. & Zepf, M. (2008). Active manipulation on the spatial energy distribution of laser-accelerated proton beams. *Phys. Rev. E* **76**, 065401(R).

Chekhlov, O.V., Bates, P.K., Cardoso, L., Collier, J.L., Danson, C.N., Hancock, S., Hernandez-Gomez, C., Matousek, P., Neely, D., Notley, M., Ross, I.N. & Shaikh, W. (2006). 35 J Boradband Femtosecond OPCPA System. *Opt. Lett.* **31**, 3665.

Clarke, R. J., Bellei, C., Carroll, D. C., Dromey, B., Green, J. S., Kneip, S., Markey, K., Mckenna, P., Murphy, W., Nagel, S., Simpson, P. T., Kar, S., Willingale, L. & Zepf, M. (2008). Nuclear activation as a high dynamic range diagnostic of laser-plasma interactions *Nucl. Instru. Meth. Phys. Res. A* **585**, 117–120.

Clarke, R.J., Brummitt, P.A., Collier, J.L., Danson, C.N., Edwards, R.D., Hatton, P.E., Hawkes, S.J., Heathcote, R., Hernandez-Gomez, C., Holligan, P., Hutchinson, M.H.R., Kidd, A. K., Ledingham, K.W.D., Lester, W.J., Mckenna, P., Neely, D., Neville, D.R., Norreys, P.A., Pepler, D.A., Winstone, T.B., Wyatt, R.W.W., Wright, P.N.M. & Wyborn, B.E. (2006). Radiological characterisation of photon radiation from ultra high intensity laser plasma and nuclear interactions. *J. Radiolog. Protection* **26**, 3, 277–286.

Guenther, M. M., Britz, A., Clarke, R. J., Harres, K., Hoffmeister, G., Nuernberg, F., Otten, A., Pelka, A., Roth, M. & Vogt, K. (2013). NAIS: Nuclear activation based imaging spectroscopy. *Rev. Sci. Instru.* **84**, 073305.

https://doi.org/10.1017/S026303461400038X Published online by Cambridge University Press

Hernandez-Gomez, C., Brummitt, P.A., Canny, D.J., Clarke, R.J., Collier, J., Danson, C.N., Dunne, A.M., Fell, B.A., Frackiewicz, J., Hancock, S. Hawkes, S., Heathcote, R., Holligan, P., Hutchinson, M.H.R., Kidd, A., Lester, Wj., Musgrave, I.O., Neely, D., Neville, D.R., Norreys, P.A., Pepler, D.A., Reason, C.J., Shaikh, W., Winstone, T.B. & Wyborn, B.E. (2006). Vulcan petawatt-operation and development. *J. Phys. IV France* **133**, 555–559.

Kneip, S., Bellei, C., Cheklov, O., Clarke, R.J., Delerue, N., Divall, E.J., Doucas, G., Ertel, K., Fiuza, F., Fonseca, R., Foster, P., Hawkes, S. J., Heathcote, R., Hooker, C.J., Krushelnick, K., Mangles, S.P.D., Martins, S.F., Nagel, S.R., Najmudin, Z., Palmer, C.A. J., Phuoc, K..Ta, Rajeev, P., Schreiber, J., Silva, L.O., Streeter, M.J.V., Urner, D. & Vieira, J. (2011). Study of near-GeV acceleration of electrons in a non-linear Plasma wave driven by a self-guided laser pulse. *Plasma Phys. Contr. Fusion* **53**, 014008.

Ledingham, K.W.D., Allott, R., Beg, F.N., Clark, E., Clark, R.J. Cresswell, A.J., Dangor, A.E., Krushelnick, K., Machacek, A.C., Magill, J., Mccanny, T., Neely, D., Norreys, P.A., Sanderson, D.C.W., Santala, M.I.K., Singhal, Rp., Spencer, I., Tatarakis, M., Wark, J.S., Watts, I. & Zepf, M. (2000). Photonuclear physics when a multiterawatt laser pulse interacts with solid targets. *Phys. Rev. Lett.* **84**, 5.

Nuernberg, F., Blazevic, A., Brambrink, E., Carroll, D.C., Flippo, K., Gautier, D.C., Geissel, M., Harres, K., Hegelich, B.M., Lundh, O., Markey, K., Mckenna, P., Neely, D., Schollmeier, M., Schreiber, J., Roth, M. (2009). Radiochromic film imaging spectroscopy of laser accelerated proton beams. *Rev. Sci. Instru.* **80**, 0333.

Robson, L., Clarke, R.J., Ledingham, K.W.D., Lindau, F., Lundh, O., Mccanny, T., Mckenna, P., Mora, P., Neely, D., Simpson, P.T., Wahlstrom, C.-G. & Zepf, M. (2007). Scaling of proton acceleration driven by petawatt-laser-plasma interactions. *Nature Phys.* **3**, 58–62.

Santala, M.I.K., Allott, R., Beg, F.N., Clark, E.L., Clarke, R.J., Dangor, A.E., Krushelnick, K., Ledingham, K.W.D., Machacek, A.C., Mccanny, T., Norreys, P.A., Spencer, I., Tatarakis, M., Watts, I. & Zepf, M. (2001). Production of radioactive nuclides by energetic protons generated from intense laser-plasma interactions. *Appl. Phys. Lett.* **78**, 19.

Yuan, X.H., Borghesi, M., Carroll, D.C., Clarke, R.J., Evans, R.G., Fuchs, J., Gallegos, P., Lancia, L., Mckenna, P., Neely, D., Robinson, A.P. L., Romagnani, L., Sarri, G., Quinn, K., Quinn, M.N. & Wilson, P.A. (2010). Effect of self generated magnetic fields on fast electron beam divergence in solid targets. *New J. Phys.* **12**, 063018.

Ziener, C., Divall, E.J., Foster, P.S., Hooker, C.J., Hutchinson, M.H.R., Langley, A.J. & Neely, D. (2003). Specular reflectivity of plasma mirrors as a function of intensity, pulse duration and angle of incidence. *J. Appl. Phys.* **93**, 1.

https://doi.org/10.1017/S026303461400038X Published online by Cambridge University Press